

# Facile Synthesis of Spirocyclic Aromatic Hydrocarbon Derivatives Based on *o*-Halobiaryl Route and Domino Reaction for Deep-Blue Organic Semiconductors

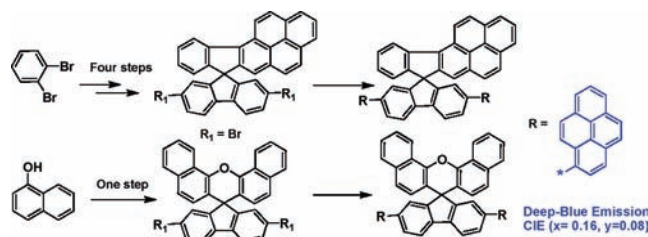
Feng Liu,<sup>†</sup> Ling-Hai Xie,<sup>†</sup> Chao Tang,<sup>†</sup> Jing Liang,<sup>†</sup> Qing-Quan Chen,<sup>†</sup> Bo Peng,<sup>†</sup> Wei Wei,<sup>\*,†</sup> Yong Cao,<sup>‡</sup> and Wei Huang<sup>\*,†</sup>

Jiangsu Key Lab for Organic Electronics & Information Displays and Institute of Advanced Materials (IAM), Nanjing University of Posts & Telecommunications (NUPT), 9 Wenyuan Road, Nanjing 210046, China, and Institute of Polymer Optoelectronic Materials and Devices, South China University of Technology, Guangzhou 510640, China

wei-huang@njupt.edu.cn; iamww@fudan.edu.cn

Received June 24, 2009

## ABSTRACT



Conventional *o*-halobiaryl and one-pot tandem protocols have been developed to synthesize naphthalene- and pyrene-containing spirofluorenes. Two pyrene substituents were installed using a Suzuki cross-coupling reaction to produce a series of spirofluorene-functionalized polycyclic aromatic hydrocarbon derivatives, DPSBFF, DPSIPF, DPSDBXF, and DPSFX. A preliminary spin-coated device based on DPSFX:PVK blends exhibits a low turn-on voltage of 4.3 V and deep-blue emission with a current efficiency of 1.1 cd/A.

Polycyclic aromatic hydrocarbons (PAHs) are important planar organic semiconductors for high-performance OFETs.<sup>1,2</sup> However, they are not favored in OLEDs due to the large red-shifted emission as well as concentration-quenching effect from solution to solid state. Recently, pyrene-functionalized materials were proven to be promising blue emitters because of their high photoluminescence efficiency, high carrier mobility, and improved hole-injecting ability.<sup>3</sup>

On the other hand, bulky spirofluorene building blocks, especially spirobifluorene (SBF), are widely used in optoelectronic materials due to their unique steric hindrance effect.<sup>4</sup> The introduction of spirofluorene frameworks into organic semiconductors could increase the thermal and morphological stability as well as carrier mobility.<sup>5</sup> Although novel spirofluorenes are continuously reported, there are few reports on spiro-functionalized polycyclic aromatic hydrocarbon (SPA) derivatives. Incorporation of PAHs into cruciform spirobifluorenes is an effective method to control the  $\pi$ - $\pi$  stacking interactions, which significantly impacts the emission behaviors of devices.

<sup>†</sup> Nanjing University of Posts & Telecommunications.

<sup>‡</sup> South China University of Technology.

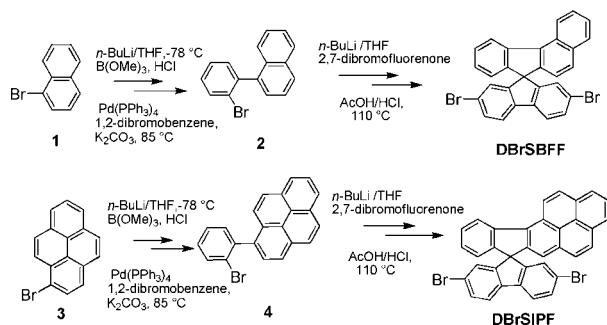
(1) Wu, J. S.; Pisula, W.; Mullen, K. *Chem. Rev.* **2007**, *107*, 718–747.

(2) Zaumseil, J.; Sirringhaus, H. *Chem. Rev.* **2007**, *107*, 1296–1323.

So far, there have been several synthetic protocols to prepare spirofluorenes in the literature. One of the most popular protocols is the *o*-halobiaryl route, in which an *o*-halobiaryl anion first attacks fluorenone to form a corresponding tertiary alcohol and is then followed by Friedel–Crafts cyclization.<sup>6</sup> With this method, various specified spirofluorenes could be obtained by designing symmetric and asymmetric *o*-halobiaryls. Yet this method requires laborious multistep reactions.<sup>7</sup> Recently, a one-pot tandem preparation strategy for spirofluorenes was reported.<sup>8,9</sup> Spiro[fluorene-9,9'-xanthene] (SFX) was occasionally obtained in the preparation of 4,4'-(9-fluorenylidene)diphenol.<sup>8</sup> To the best of our knowledge, spiro[dibenzo[*c,h*]xanthene-7,9-fluorene] (SDBXF) is still unexplored. In this communication, we prepared a series of spirocycle aromatic hydrocarbons (SCAHs), naphthalene- and pyrene-containing spirofluorenes, via conventional *o*-halobiaryls and one-pot tandem protocols. Their pyrene-functionalized derivatives are excellent blue light-emitting materials in solution-processable devices.

The asymmetric naphthalene- and pyrene-containing spirofluorene building blocks were synthesized using the *o*-bromobiaryl route as shown in Scheme 1. *o*-Bromobiaryls

**Scheme 1.** Synthesis Routes of DBrSBFF and DBrSPPF via the *o*-Bromodiaryl Intermediates

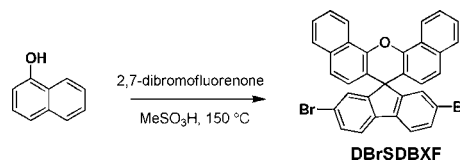


**2** and **4** were synthesized via the Suzuki coupling reaction. This was followed by addition of 2,7-dibromofluorenone under *n*-BuLi conditions affording the corresponding tertiary alcohols. The crude products underwent dehydration cyclization to obtain the key SCAH building blocks 2',7'-dibromospiro[benzo[*c*]fluorene-7,9'-fluorene] (DBrSBFF) and 2,7-dibromospiro[fluorene-9,7'-indeno[1,2-*a*]pyrene] (DBrSPPF).

According to our previous one-pot tandem protocol,<sup>8</sup> 2,7-dibromofluorenone and naphthalen-1-ol were stirred together under the conditions of methylsulfonic acid at 150 °C, and

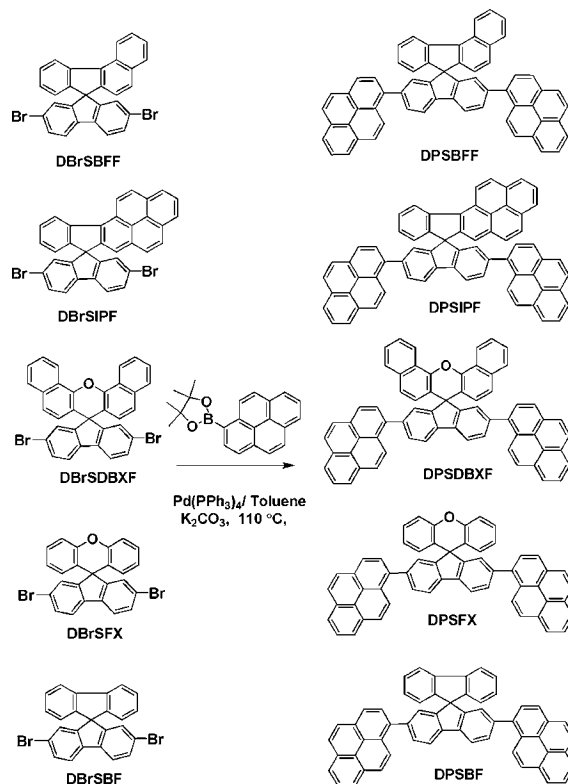
then 2',7'-dibromospiro[dibenzo[*c,h*]xanthene-7,9-fluorene] (DBrSDBXF) was obtained in nearly stoichiometric yields, as shown in Scheme 2.

**Scheme 2.** One-Pot Procedures for DBrSDBXF



This key intermediate was reacted with 4,4,5,5-tetramethyl-2-(pyren-1-yl)-1,3,2-dioxaborolane using the Suzuki coupling reaction to afford the 2,7-dipyrene-functionalized organic semiconductors (Scheme 3). <sup>1</sup>H NMR and MALDI-TOF-

**Scheme 3.** Synthesis of Pyrene-Functionalized Final Products



MS were used to characterize their structures (Supporting Information). Among these SPAHs, DPSBF was used for comparison.<sup>10</sup> DPSBFF and DPSIPF possess asymmetric SCAHs. DPSFX and DPSDBXF contain an oxygen atom in the SCAHs.

(3) (a) Liu, F.; Tang, C.; Chen, Q. Q.; Shi, F. F.; Wu, H. B.; Xie, L. H.; Peng, B.; Wei, W.; Cao, Y.; Huang, W. *J. Phys. Chem. C* **2009**, *113*, 4641–4647. (b) Liu, F.; Tang, C.; Chen, Q. Q.; Li, S. Z.; Wu, H. B.; Xie, L. H.; Peng, B.; Wei, W.; Cao, Y.; Huang, W. *Org. Electron.* **2009**, *10*, 256–265. (c) Liu, F.; Lai, W. Y.; Tang, C.; Wu, H. B.; Chen, Q. Q.; Peng, B.; Wei, W.; Huang, W.; Cao, Y. *Macromol. Rapid Commun.* **2008**, *29*, 659–664. (d) Tang, C.; Liu, F.; Xia, Y. J.; Xie, L. H.; Wei, A.; Li, S. B.; Fan, Q. L.; Huang, W. *J. Mater. Chem.* **2006**, *16*, 4074–4080. (e) Tang, C.; Liu, F.; Xia, Y. J.; Lin, J.; Xie, L. H.; Zhong, G. Y.; Fan, Q. L.; Huang, W. *Org. Electron.* **2006**, *7*, 155–162.

(4) (a) Saragi, T. P. I.; Spehr, T.; Siebert, A.; Fuhrmann-Lieker, T.; Salbeck, J. *Chem. Rev.* **2007**, *107*, 1011–1065. (b) Chiang, C. L.; Shu, C. F.; Chen, C. T. *Org. Lett.* **2005**, *7*, 3717–3720.

(5) Wu, C. C.; Liu, W. G.; Hung, W. Y.; Liu, T. L.; Lin, Y. T.; Lin, H. W.; Wong, K. T.; Chien, Y. Y.; Chen, R. T.; Hung, T. H.; Chao, T. C.; Chen, Y. M. *Appl. Phys. Lett.* **2005**, *87*, 052103.

The absorption spectra of DPSBF and DPSFX exhibit quite similar profiles (Figure 1) since the SPAHs possess

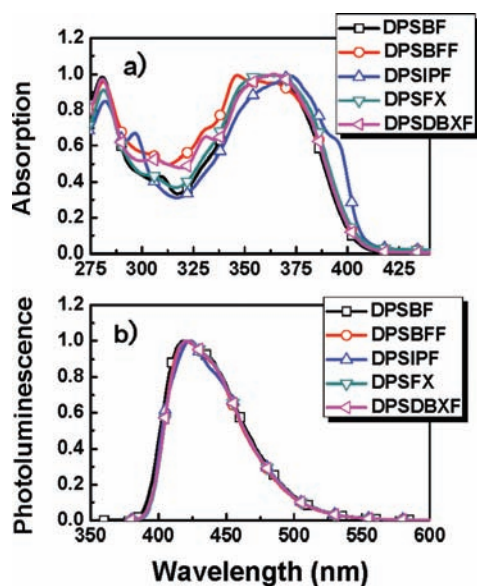


**Figure 1.** (a) Absorption spectra of SPAHs in dilute  $\text{CHCl}_3$  solution ( $10^{-6}$  M). (b) Photoluminescence spectra of SPAHs in dilute  $\text{CHCl}_3$  solution ( $10^{-6}$  M) excited using the maximum absorption wavelength.

the same main backbone of pyrene–fluorene–pyrene. The oxygen atom in the SCAH has a very weak effect on main chain conjugation and electronic structure of the materials. The absorption of DPSDBXF is close to DPSBFF, but the latter possesses an obvious new peak at 340 nm which can be attributed to a covalently conjugated connection between the naphthalene and benzene groups in the SCAH. DPSIPF is different from the other SPAHs, with a max absorption peak at 371 nm and an absorption shoulder at about 400 nm, suggesting that by enlarging the conjugation of the SCAH, the electronic structure of the conjugated backbone could be affected. The photoluminescence spectra of these molecules are nearly identical with the peak at 422 nm. DPSIPF shows a little difference, because of its large conjugated SCAH. The electrochemical behaviors of these

materials were investigated by cyclic voltammetry. The onset oxidation peaks ( $E_{\text{ox}}$ ) for DPSBF, DPSFX, DPSDBXF, DPSBFF, and DPSIPF were 0.84, 0.88, 0.82, 0.81, and 0.79 eV, respectively. Their HOMO energy levels were estimated to be  $-5.55$ ,  $-5.59$ ,  $-5.53$ ,  $-5.52$ , and  $-5.50$  eV.<sup>11</sup> For DPSBF, DPSBFF, and DPSIPF, while increasing the conjugation of the SCAH, the HOMO energy level slightly increased. From their UV–vis absorption edges, their band gap ( $\Delta E_{\text{abs}}$ ) was determined to be 2.98 eV. Thus, the LUMO was calculated. The corresponding data are summarized in Table 1.

**Table 1.** Physical Properties of Target Molecules

molecule	$\lambda_{\text{abs,max}}$ (nm)	$\lambda_{\text{PL,max}}$ (nm)	$\Delta E_{\text{abs}}$ (eV)	abs edge (nm)	HOMO (eV)	LUMO <sup>a</sup> (eV)
DPSBF	364	421	2.98	416	$-5.55$	$-2.57$
DPSBFF	364	422	2.98	416	$-5.52$	$-2.54$
DPSIPF	371	424	2.98	416	$-5.50$	$-2.52$
DPSFX	364	422	2.98	416	$-5.59$	$-2.61$
DPSDBXF	365	422	2.98	416	$-5.53$	$-2.55$

<sup>a</sup> LUMO = HOMO  $- \Delta E_{\text{abs}}$  (band gap).

Quantum chemistry was employed to study the electronic structure of these materials. The molecules were optimized using the DFT/B3LYP method at a 6-31G level; the Zindo/S method was used to estimate the transition energies ( $\Delta E_t$ ) and the oscillator strength ( $I$ ). The data are summarized in Table 2.

**Table 2.** Calculated HOMO, LUMO, and the Energy Gap ( $\Delta E$  /eV) by B3LYP/6-31G Method

molecule	HOMO	LUMO	$\Delta E_{\text{calc}}$	$\Delta E_t$	intensity (meV)	H <sup>hole</sup> (meV)	H <sup>electron</sup> (meV)
DPSBF	$-5.136$	$-1.667$	3.469	3.182	1.904	154	220
DPSBFF	$-5.133$	$-1.667$	3.466	3.173	1.896	156	218
DPSIPF	$-5.132$	$-1.724$	3.408	3.116	0.702	101	126
DPSFX	$-5.167$	$-1.700$	3.467	3.179	1.915	152	223
DPSDBXF	$-5.161$	$-1.697$	3.464	3.179	1.909	157	226

DPSFX and DPSDBXF show lower HOMO/LUMO than DPSBF due to the introduction of an oxygen atom. DPSIPF shows lower LUMO compared to DPSBF, indicating that the SCAH with more extensive conjugation could increase the electron affinity of the materials. In the Zindo/S calculations, DPSBF, DPSFX, DPSDBXF, and DPSBFF show similar transition energies and oscillator strength. DPSIPF shows lower transition energy and smaller oscillation intensity. The second lowest transition of DPSIPF shows an intensity of 1.980 (Supporting Information). Combined with the absorption study, we could ascribe the 400 nm absorption

(11) Sun, Q. J.; Wang, H. Q.; Yang, C. H.; Li, Y. F. *J. Mater. Chem.* **2003**, *13*, 800–806.

(6) (a) Yu, W. L.; Pei, J.; Huang, W.; Heeger, A. J. *Adv. Mater.* **2000**, *12*, 828–831. (b) Xie, L. H.; Fu, T.; Hou, X. Y.; Tang, C.; Hua, Y. R.; Wang, R. J.; Fan, Q. L.; Peng, B.; Wei, W.; Huang, W. *Tetrahedron Lett.* **2006**, *47*, 6421–6424. (c) Xie, L. H.; Hou, X. Y.; Hua, Y. R.; Huang, Y. Q.; Zhao, B. M.; Liu, F.; Peng, B.; Wei, W.; Huang, W. *Org. Lett.* **2007**, *9*, 1619–1622. (d) Londenberg, J.; Saragi, T. R. L.; Suske, I.; Salbeck, J. *Adv. Mater.* **2007**, *19*, 4049–4053.

(7) (a) Luo, J.; Zhou, Y.; Niu, Z. Q.; Zhou, Q. F.; Ma, Y. G.; Pei, J. *J. Am. Chem. Soc.* **2007**, *129*, 11314–11315. (b) Chen, C. T.; Wei, Y.; Lin, J. S.; Moturu, M.; Chao, W. S.; Tao, Y. T.; Chien, C. H. *J. Am. Chem. Soc.* **2006**, *128*, 10992–10993.

(8) Xie, L. H.; Liu, F.; Tang, C.; Hou, X. Y.; Hua, Y. R.; Fan, Q. L.; Huang, W. *Org. Lett.* **2006**, *8*, 2787–2790.

(9) (a) Tseng, Y. H.; Shih, P. I.; Chien, C. H.; Dixit, A. K.; Shu, C. F.; Liu, Y. H.; Lee, G. H. *Macromolecules* **2005**, *38*, 10055–10060. (b) McFarlane, S. L.; Coumont, L. S.; Piercey, D. G.; McDonald, R.; Veinot, J. G. C. *Macromolecules* **2008**, *41*, 7780–7782.

(10) Tao, S. L.; Peng, Z. K.; Zhang, X. H.; Wang, P. F.; Lee, C. S.; Lee, S. T. *Adv. Funct. Mater.* **2005**, *15*, 1716–1721.

shoulder to the lowest transition ( $S_0-S_1$ ) and the maximum absorption at 371 nm to the second lowest transition ( $S_0-S_2$ ). Thus, when the conjugation of the SCAH reached a certain extent, the frontier orbital and transition state of the material would be affected. Actually, the LUMO of DPSIPF is dominated by the SCAH, which is different from other materials (Supporting Information).

The Marcus theory was used to evaluate charge migration of these materials,<sup>12</sup> and the data are summarized in Table 2 (Supporting Information). Reorganization energies for hole and electron are quite similar for DPSBF, DPSFX, DPSDBXF, and DPSBFF. However, DPSIPF shows a much smaller value for both hole and electron. Although they have the same backbone, the conjugated SCAH for DPSIPF has a much stronger effect in affecting the electronic structure, leading to a decreased reorganization energy, and providing a better carrier transporting properties.

A spin-coated OLED device was fabricated by using DPSFX (5 wt %): PVK blends as the active layer. PBD (30 wt % compared to PVK) was added to increase electron mobility.<sup>13</sup> The device shows a deep-blue emission with CIE 1931 coordinates of ( $x = 0.16$ ,  $y = 0.08$ ). The electroluminescence is very close to that of DPSFX in solution. The turn-on voltage is 4.3 V and the maximum brightness is over 2000  $\text{cd/m}^2$ . The peak current efficiency reaches 1.1  $\text{cd/A}$ . Basic device performance shows that DPSFX is a promising light emitting material. Its potential could be fully explored by optimizing the device structure or using a vacuum deposition device fabrication method (Figure 2).

In conclusion, we have explored two different protocols to synthesize naphthalene- and pyrene-containing spirocycle aromatic hydrocarbons for novel nonplanar organic semi-

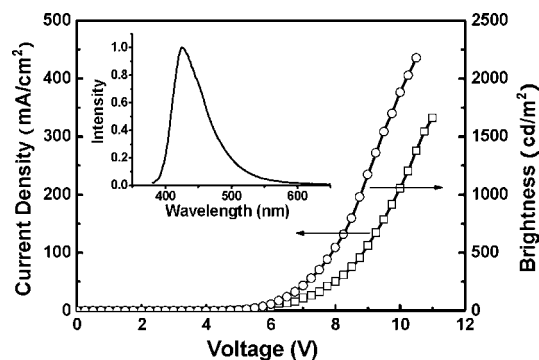


**Figure 2.** Performance of device with the configuration: [ITO/PEDOT:PSS (40 nm)/emitter (80 nm)/CsF (2 nm)/Al (90 nm)].

conductors. They show deep-blue emission and interesting device performance. Their electronic structure was studied by quantum chemistry and the carrier migration properties were analyzed by the Marcus theory. These preliminary results show that  $\pi$ -conjugated spirofluorene-functionalized PAHs are a promising family of organic semiconductors.

**Acknowledgment.** For financial support for this work, we thank the “973” project (2009CB930600), NNSFC (Grant Nos. 20704023, 60876010, 60706017, and 20774043), the Key Project of Chinese Ministry of Education (Nos. 208050 and 707032), and the NSF of the Education Committee of Jiangsu Province (Grant Nos. 07KJB150082, BK2008053, SJ209003, and TJ207035).

**Supporting Information Available:** Detailed synthetic procedures, NMR and MALDI-TOF-MS spectra, and molecular simulation. This material is available free of charge via the Internet at <http://pubs.acs.org>.

OL900978X

(12) Tant, J.; Geerts, Y. H.; Lehmann, M.; De Cupere, V.; Zucchi, G.; Laursen, B. W.; Bjornholm, T.; Lemaire, V.; Marcq, V.; Burquel, A.; Hennebique, E.; Gardebien, F.; Viville, P.; Beljonne, D.; Lazzaroni, R.; Cornil, J. *J. Phys. Chem. B* **2005**, *109*, 20315–20323.

(13) Jiang, C. Y.; Yang, W.; Peng, J. B.; Xiao, S.; Cao, Y. *Adv. Mater.* **2004**, *16*, 537–541.